Construction of an immune-related gene prognostic model with experimental validation and analysis of immune cell infiltration in lung adenocarcinoma

JIALEI YANG[1,2], CHAO TANG[1], CHENGXIA LI[1], XUESEN LI[1] and WENLI YANG[1,3]

[1]Institute for Cancer Medicine, School of Basic Medicine Sciences, Southwest Medical University, Luzhou, Sichuan 646000, P.R. China; [2]Department of Medical Laboratory Medicine, Dehong Prefecture People's Hospital of Yunnan Province, Mangshi, Yunnan 678400, P.R. China; [3]Department of Biochemistry and Molecular Biology, School of Basic Medicine Sciences, Southwest Medical University, Luzhou, Sichuan 646000, P.R. China

Received December 19, 2023; Accepted March 15, 2024

DOI: 10.3892/ol.2024.14430

Abstract. There is a correlation between tumors and immunity with the degree of immune cell infiltration in tumors being closely related to tumor growth and progression. Therefore, the present study identified immune-related prognostic genes and evaluated the immune infiltration level in lung adenocarcinoma (LUAD). This study performed Kyoto Encyclopedia of Genes and Genomes, Gene Ontology, and Gene Set Enrichment Analysis (GSEA) enrichment analyses on differential immune-associated genes. A risk model was created and validated using six immune-related prognostic genes. Reverse transcription-quantitative PCR was used to assess the prognostic gene expression in non-small cell lung cancer cells. Immune cell infiltration in LUAD was analyzed using the CIBERSORT method. Single sample GSEA was used to compare Tumor Immune Dysfunction and Exclusion (TIDE) scores between high and low-risk groups and to assess the activation of thirteen immune-related pathways. Multifactor Cox proportional hazards model analysis identified six prognostic risk genes (*S100A16, FURIN, FGF2, LGR4, TNFRSF11A* and *VIPR1*) to construct a risk model. The survival and receiver operating characteristic curves indicated that patients with higher risk scores had lower overall survival rates. The expression levels of prognostic genes *S100A16, FURIN, LGR4, TNFRSF11A* and *VIPR1* were significantly increased in LUAD. B cells naive, plasma cells, T cells CD4 memory activated, T cells follicular helper, T cells regulatory, NK cells activated, macrophages M1, macrophages M2, and Dendritic cells resting cells showed elevated expression in LUAD. The prognostic genes were differentially associated with individual immune cells. Immune-related function scores, such as those for antigen presenting cell (APC) co-stimulation, APC co-inhibition, check-point, Cytolytic-activity, chemokine receptor, parainflammation, major histocompatibility complex-class-I, type-I-IFN-reponse and T-cell-co-inhibition, were higher in the high-risk group compared with the low-risk group. Furthermore, the TIDE score of the high-risk group was significantly lower than the low-risk group. This immune-related gene prognostic model has the potential to predict the prognosis of LUAD patients, supporting the development of a personalized clinical diagnosis and treatment plan.

Correspondence to: Professor Wenli Yang, Institute for Cancer Medicine, School of Basic Medical Sciences, Southwest Medical University, 1 Section 1, Xianglin Road, Longmatan, Luzhou, Sichuan 646000, P.R. China
E-mail: ywl0621@swmu.edu.cn

Key words: lung adenocarcinoma, immune-related genes, prognosis, immune cell infiltration, bioinformatics

Introduction

Lung cancer is the second most common malignant tumor worldwide (1). Lung cancer is primarily divided into non-small cell lung cancer (NSCLC) and small cell lung cancer based on histopathological features (2). Lung adenocarcinoma (LUAD) accounts for >40% of NSCLC (3) and is a common type of lung cancer tissue (4). LUAD patients are typically older when diagnosed, at a later disease stage, possess a worse prognosis, and have a 5-year survival rate <20% (5). Surgery, radiotherapy and chemotherapy are the primary treatment modalities for lung cancer. However, their efficacy is often limited in patients with metastatic lung cancer. Therefore, an in-depth exploration of the molecular mechanisms related to the pathogenesis of LUAD could support the search for optimized approaches to early diagnosis and treatment targeting specific genes.

The role of the immune system in the occurrence and development of tumors is complex. It can eliminate tumor cells in specific tissues, establish an inflammatory environment that prevents tumorigenesis by removing pathogens and inflammation, and promote tumor growth through immunoediting amongst other methods (6). Moreover, tumor cells can adopt various methods to evade immune system attack, including changing surface antigens and inhibiting immune cell activity. The primary components of tumor immunity are an immunosuppressive tumor microenvironment (TME) and dysfunctional anti-tumor T cells (7). The complex surroundings around the tumor, including components such as molecules, blood vessels, and other non-tumor cells, are known as the TME and influence both the anti-tumor immune response and immunotherapy effectiveness (8). Development in immunotherapy have been remarkably successful in treating certain cancers. In LUAD, patients were administered immune checkpoint inhibitors (ICIs) to target programmed cell death 1, programmed cell death ligand 1 and cytotoxic T lymphocyte antigen 4 which improved survival (9). However, there are some issues with immunotherapy, such as acquired resistance and severe side effects (10). A previous study reported that tumor cell and TME interaction in spatiotemporal dynamics was essential for tumor progression (11). Thus, tumor growth promotes the development of immunological tolerance in the body, weakening the therapeutic effect of ICIs (12). Not every lung adenocarcinoma patient responds to ICI treatment due to the effects of immune tolerance. Moreover, the abnormal expression of tumor immune-related genes in tumor escape has become a novel direction of focus in tumor research (13). However, to the best of our knowledge, only a few reports exist on how abnormal immune-related genes affect lung adenocarcinoma prognosis and immune cell infiltration. Therefore, elucidating the immune genes associated with lung adenocarcinoma prognosis and constructing a LUAD prognosis model based on immune cell infiltration in such patients, could have clinical value.

In the present study, LUAD-related data were retrieved from The Cancer Genome Atlas (TCGA) database and bioinformatics were used to analyze the immune-related genes significantly linked with the prognosis of LUAD patients. An immune-related genes prognostic model was constructed and its independent prediction power was assessed. The study also used reverse transcription-quantitative (RT-qPCR) to analyze immune-related prognostic gene expression while evaluating immune cell infiltration and function levels in LUAD. Thus, an immune-related prognostic risk model was developed for LUAD based on disease transcriptomics, offering novel targets for therapeutic immunotherapy.

Materials and methods

Data sources. The RNA sequencing and clinical data of 535 LUAD samples and 59 normal tissues were retrieved from the TCGA database (http://www.cancer.gov/). The gene expression data were corrected in batches and those with missing information regarding clinical features were eliminated. Finally, there were 522 LUAD samples and normal tissues. A total of 2,483 immune-related genes were downloaded from the Immunology Database and Analysis Portal (ImmPort) database (http://www.immport.org/). LM22 marker genes were downloaded from the CIBERSORT website (https://cibersortx.stanford.edu). The Human Protein Atlas (https://www.proteinatlas.org) database was used to retrieve prognostic immune-related gene protein expression data. The TIDE algorithm was used to predict responses to ICIs therapy (14).

Screening of immune-related differential genes and enrichment analysis. Differential analysis was performed across all LUAD patient genes using the limma package (https://bioinf.wehi.edu.au/limma/), with fdrFilter=0.05 and logFCfilter=2, followed by construction of the differential gene volcano diagram with graphics (https://www.R-project.org/). The differentially expressed immune-related genes were obtained by assessing the intersection of the differentially expressed genes (DEGs) with 2483 immune-related genes with the Venn diagram depicting the intersection results by venn package (https://CRAN.R-project.org/package=venn). Gene Set Enrichment Analysis (GSEA) (15), Gene Ontology (GO) and Kyoto Encyclopedia of Genes and Genomes (KEGG) (https://ggplot2.tidyverse.org) enrichment analysis were performed on the differentially expressed immune-related genes previously identified. Univariate Cox regression analysis was used to identify the immune-related genes associated with prognosis and DEGs with $P<0.05$ were included in the multifactor Cox proportional hazards model analysis to obtain the immune-related genes which were subsequently used to construct the prognostic model.

Construction and analysis of prognostic risk models. The expression levels of the prognostic immune-related genes, identified by the aforementioned multivariate Cox regression analyses, were multiplied using the coefficients obtained from their respective multivariate Cox regression analyses to determine the risk score of each patient. A prognostic risk model was then constructed using multifactor Cox proportional hazards model analysis. Patients were divided into high and low-risk groups with the median risk score as the cutoff value, followed by the plotting of the Kaplan-Meier survival curve (https://CRAN.R-project.org/package=survival), receiver operating characteristic (ROC) curve (16) and nomogram (https://CRAN.R-project.org/package=rms). Univariate and multivariate Cox regression analyses were also performed for the hazard ratio (HR) of the risk score and clinical characteristics including age, gender, stage and, tumor (T), node (N) and metastasis (M) scores.

Immune infiltration analysis in LUAD. The LUAD immune cells of LM22 marker genes were analyzed using the CIBERSORT algorithm, with $P<0.05$ being considered to indicate a statistically significantly difference. The Wilcox.test was used to assess the differences in immune cell expression in LUAD, and a differential heatmap of lung adenocarcinoma immune cells was drawn. Student's t-test was used to evaluate differences in immune cells and the relationship between prognostic genes and immune cells in high and low-risk groups. Single sample GSEA was used to compare Tumor Immune Dysfunction and Exclusion (TIDE) scores between high and low-risk groups and to determine immune-related functional activity.

Cell culture. Human normal lung epithelial MRC5 cells and human NSCLC A549 and H1975 cells were purchased from The Cell Bank of Type Culture Collection of the Chinese Academy of Sciences. The cells were cultured in DMEM high glucose (H) medium containing 10% fetal bovine serum and incubated at 37˚C with 5% CO_2, with the medium replaced every 2-3 days.

RNA extraction and RT-qPCR. Total RNA was extracted from MRC5, A549 and H1975 cells using TRIzol® (Invitrogen;

Table I. Sequences of primers used for reverse transcription-quantitative PCR.

Gene	Sequence (5'-3')
S100A16	F: CAGCCTGGTCAAGAACAAGAT
	ATGATTGGCATCCAGGTTC
FURIN	F: AACACTGTGCCCTGGTGGA
	R: CAGATGGCTGGGTACCAGGA
FGF-2	F: ACCGTTACCTGGCTATGAAG
	R: CCAGTTCGTTTCAGTGCC
LGR4	F: ACTCAAAGTTCTAACGCTCCAG
	R: CAGCCACAGATGCCGTAAC
TNFRSF11A	F: CCATCATCTTTGGCGTTTG
	R:CTCCTCCAGAGTCAGCAGTAAG
VIPR1	F: CATTTTGAGGATTATGGGTGC
	R: GCAGTTTCTGAAGCAGGATT
GAPDH	F: TGGAAATCCCATCACCATCT
	R: GTCTTCTGGGTGGCAGTGAT

F, forward; R, reverse.

Table II. Clinical characteristics of patients involved in the study.

Characteristics	n (%)
Age, years	
<65	223 (42.7)
≥65	280 (53.7)
Unknown	19 (3.6)
Gender	
Female	280 (53.6)
Male	242 (46.4)
T classification	
T1	172 (33.0)
T2	281 (53.8)
T3	47 (9.0)
T4	19 (3.6)
TX	3 (0.6)
N classification	
N0	335 (64.2)
N1	98 (18.8)
N2	75 (14.4)
N3	2 (0.3)
NX	11 (2.1)
Unknown	1 (0.2)
M classification	
M0	353 (67.6)
M1	25 (4.8)
MX	140 (26.8)
Unknown	4 (0.8)
Tumor stage	
I	279 (53.4)
II	124 (23.8)
III	85 (16.3)
IV	26 (5.0)
Unknown	8 (1.5)
Vital status	
Alive	167 (32.0)
Dead	355 (68.0)

T, tumor; N, node; M, metastasis.

Thermo Fisher Scientific, Inc.). RT-PCR was performed after removing genomic DNA, according to the instructions of the PrimeScript™ RT reagent kit with gDNA Eraser (Takara Biotechnology Co., Ltd.). RT-qPCR primers were designed and synthesized by Sangon Biotech Co., Ltd. (Table I). The RT-qPCR solution comprised 12.5 μl TB Green Premix Ex TaqII (Takara Biotechnology Co., Ltd.), 1.0 μl PCR forward primer (10 μM), 1.0 μl PCR reverse primer (10 μM), 2 μl RT reaction solution (complimentary DNA solution), and 8.5 μl sterilized water, for a total volume of 25 μl. The RT-qPCR reaction conditions were as follows: 95˚C for 30 sec, then 40 cycles of 95˚C for 5 sec and 60˚C for 30 sec. The relative gene expression was determined using the $2^{-\Delta\Delta Cq}$ method (17), with GAPDH used as an internal control. Each experiment was performed in triplicate.

Statistical analysis. All statistical analysis and presentations were performed using the R 4.3.0 software package (https://mirrors.tuna.tsinghua.edu.cn/CRAN/). The Wilcox.test was used to compare the differential expression of immune-related genes in LUAD and normal tissues. Immune-related genes linked with poor prognosis in LUAD were identified using multivariate Cox regression analysis. The correlation of prognostic genes and transcription factors was assessed using t-test. The comparison of the expression levels of prognostic genes in MRC5, H1975 and A549 cells was performed using one-way ANOVA with Dunnett's multiple comparisons test as the post-hoc test. Kaplan-Meier curves were used for survival analyses. P<0.05 was considered to indicate a statistically significant difference.

Results

Differential immune-related gene expression and enrichment analysis in LUAD. The clinicopathological characteristics of the 522 LUAD samples from the TCGA database were assessed (Table II). The intersection of DEGs and immune related genes in LUAD identified 505 differentially immune-related genes using logFCfilter=1 and fdrFilter=0.05 for these genes in LUAD (Fig. 1B). Among these, 338 genes were up-regulated and 167 were down-regulated (Fig. 1A and B). The volcano diagram was drawn using the DEGs. GO enrichment analysis of these differentially immune-related genes indicated that they were primarily enriched in biological processes such as 'immunoglobulin production' and 'production of molecular mediator of immune response', cellular components such as 'immunoglobulin complex' and 'external side of plasma membrane', and molecular functions such as 'antigen binding'

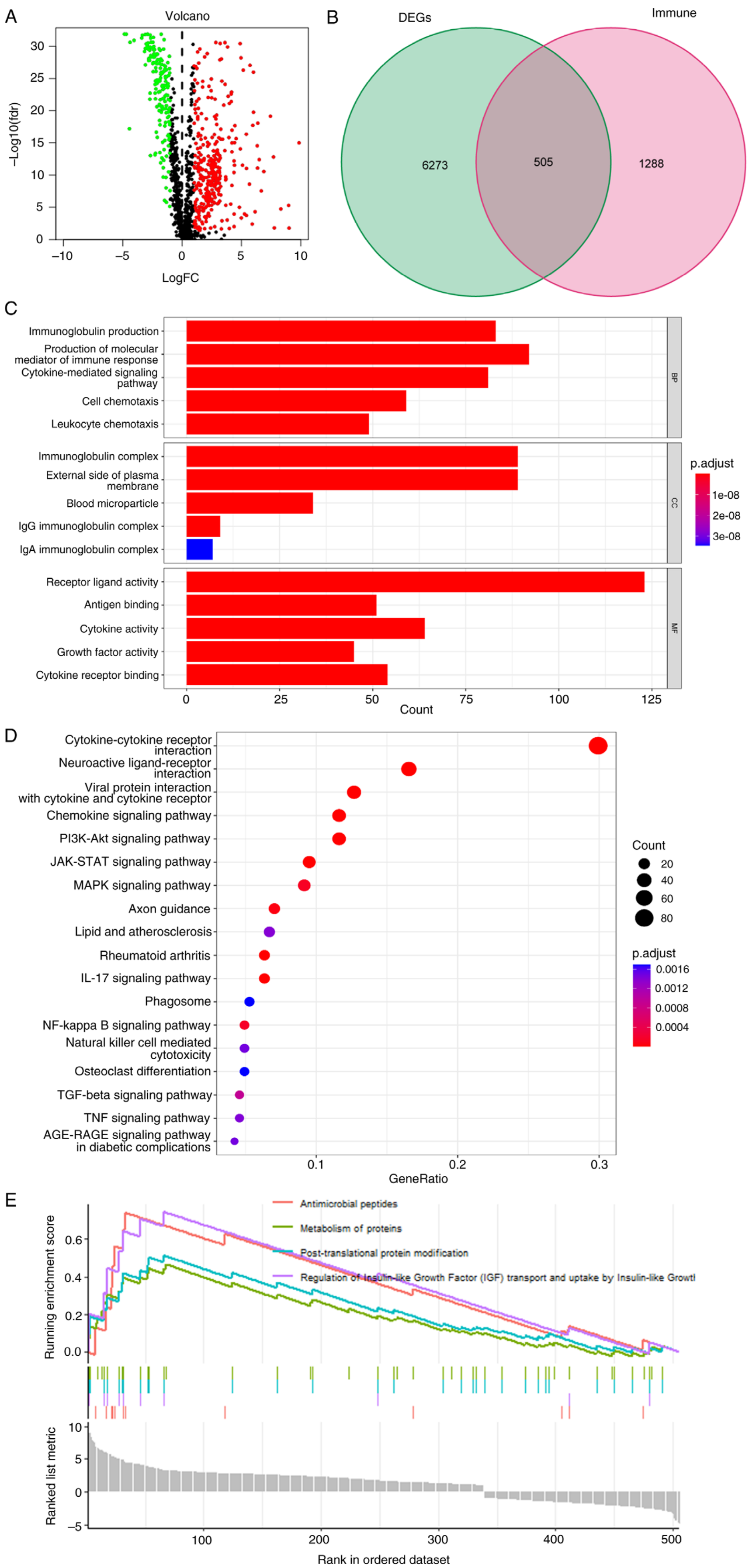

Figure 1. The differential expression and enrichment analysis of immune-related genes among lung adenocarcinoma patients. (A) Volcano map of immune-related genes. Green indicates downregulated differential immune-related genes and red indicates upregulated differential immune-related genes. (B) Immune-related gene intersection presented in a Venn diagram. (C) Gene Ontology, (D) Kyoto Encyclopedia of Genes and Genomes, and (E) Gene Set Enrichment Analysis enrichment analysis. DEGs, differently expressed genes; BP, biological processes; CC, cellular component; MF, molecular function.

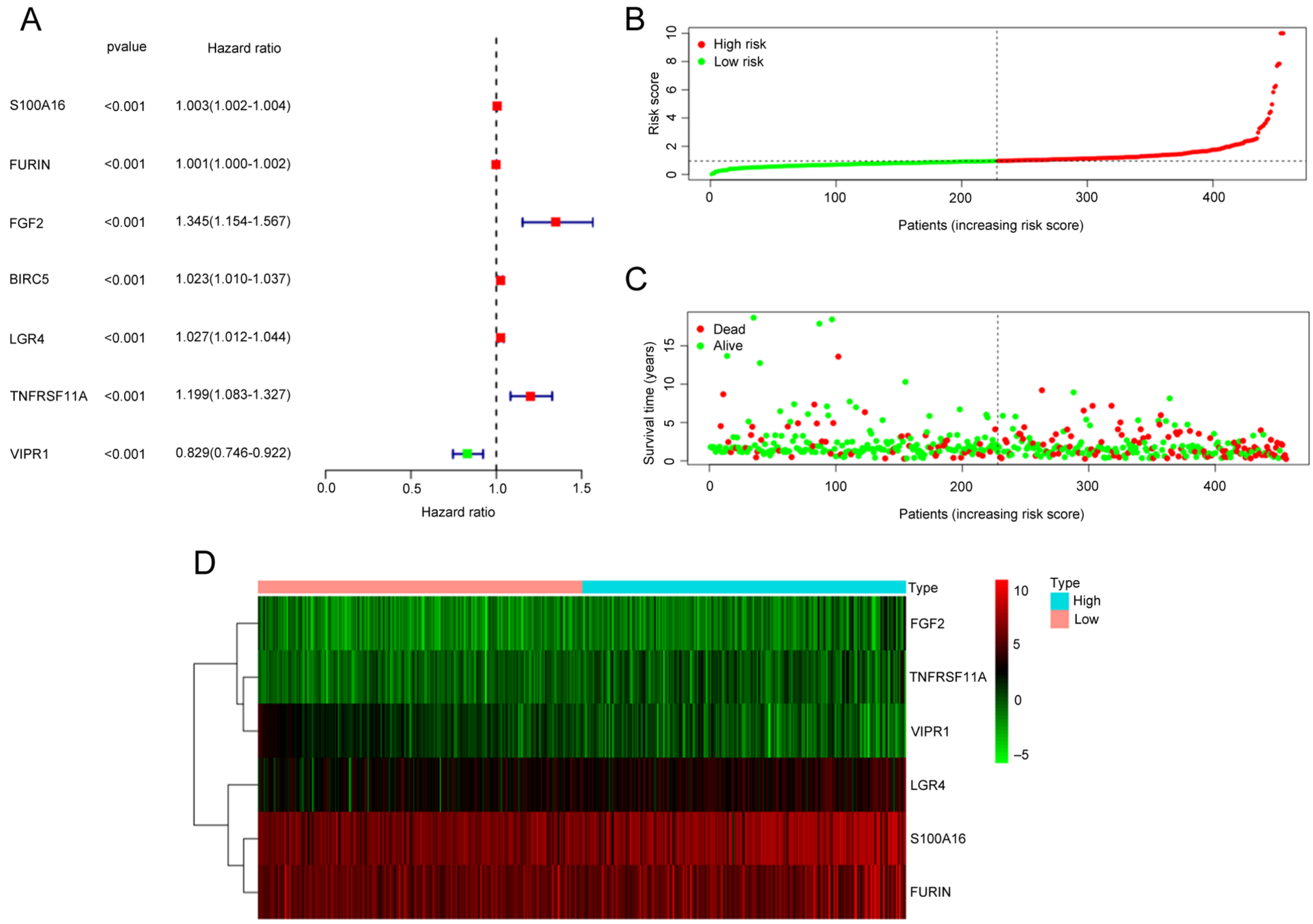

Figure 2. Prognostic model construction. (A) Forest diagram of seven differentially expressed immune genes. (B) The risk score curve with patients ordered by increased risk score. (C) The survival status diagram. (D) The survival heat map for high-risk and low-risk groups. Red represents increased expression and green indicates reduced expression.

and 'receptor ligand activity' (Fig. 1C). KEGG analysis indicated the differentially immune-related genes were mainly enriched in 'cytokine-cytokine receptor interaction', 'neuroactive receptor-ligand interaction', 'viral protein ineraction with cytokine and cytokine receptor' and 'chemokine signaling pathway' pathways (Fig. 1D). GSEA analysis demonstrated primary enrichment in 'antimicrobial peptides', 'regulation of insulin-like growth factor (IGF) transport and uptake by IGF', 'post-translational protein modification' and 'metabolism of proteins' (Fig. 1E).

Construction of a prognostic model using immune-related genes. Seven differential immune-related genes associated with prognosis were obtained using univariate Cox regression analysis (Fig. 2A). Multifactor Cox proportional hazards model analysis was performed on these seven genes, from which six prognostic genes (*S100A16*, *FURIN*, *FGF2*, *LGR4*, *TNFRSF11A* and *VIPR1*) were significantly associated with the occurrence and development of LUAD (Table III). The multivariate regression coefficients of the six prognostic immune-related genes were multiplied with their respective expression levels in each sample. Thus, the risk score of each sample was calculated as follows: risk score=*S100A16* expression level x 0.002303 + *FURIN* expression level x 0.00073 + *FGF2* expression level x 0.24979 + *LGR4* expression level x 0.015309 + *TNFRSF11A* expression level x 0.176773 - *VIPR1* expression level x 0.14724. Depending on the median risk score, the samples were differentiated into high and low-risk groups. The risk curve indicated the mortality of most patients in the high-risk group; with an increase in the patient's risk value, more patients died (Fig. 2B and C). The survival heat map indicated that the expression levels of *S100A16*, *FURIN*, *FGF2*, *LGR4* and *TNFRSF11A* gradually increased with the risk score. In contrast, *VIPR1* gene expression gradually decreased (Fig. 2D).

Independent prognostic analysis. The survival analysis of the prognostic risk model indicated that the survival time of patients with LUAD in the high-risk score group was significantly lower than those in the low-risk score group. The 5-year overall survival rate of patients in the high-risk score group was ~23%, while that of those in the low-risk score group was ~51% (Fig. 3A). The ROC curve indicated an area under the curve of 0.707 (Fig. 3B), which suggested that the prognostic model possessed strong predictive ability. A nomogram was built as a quantitative method for the six immune-related genes to predict LUAD prognosis. The nomogram point scale made it possible to assign a value to a single variable by constructing

Table III. Multifactorial Cox proportional hazard model analysis.

Gene	coef	HR	HR.95L	HR.95H	P-value
S100A16	0.002303	1.002306	1.000988	1.003626	0.000604
FURIN	0.00073	1.00073	1.000044	1.001416	0.036931
FGF2	0.24979	1.283756	1.108018	1.487367	0.000882
LGR4	0.015309	1.015427	0.998317	1.032829	0.077442
TNFRSF11A	0.176773	1.19336	1.075284	1.324403	0.000883
VIPR1	-0.14724	0.863084	0.777428	0.958178	0.005761

Coef, coefficients; HR, hazard ratio; HR.95L, the low 95% confidence interval for hazard ratio; HR.95H, the high 95% confidence interval for hazard ratio.

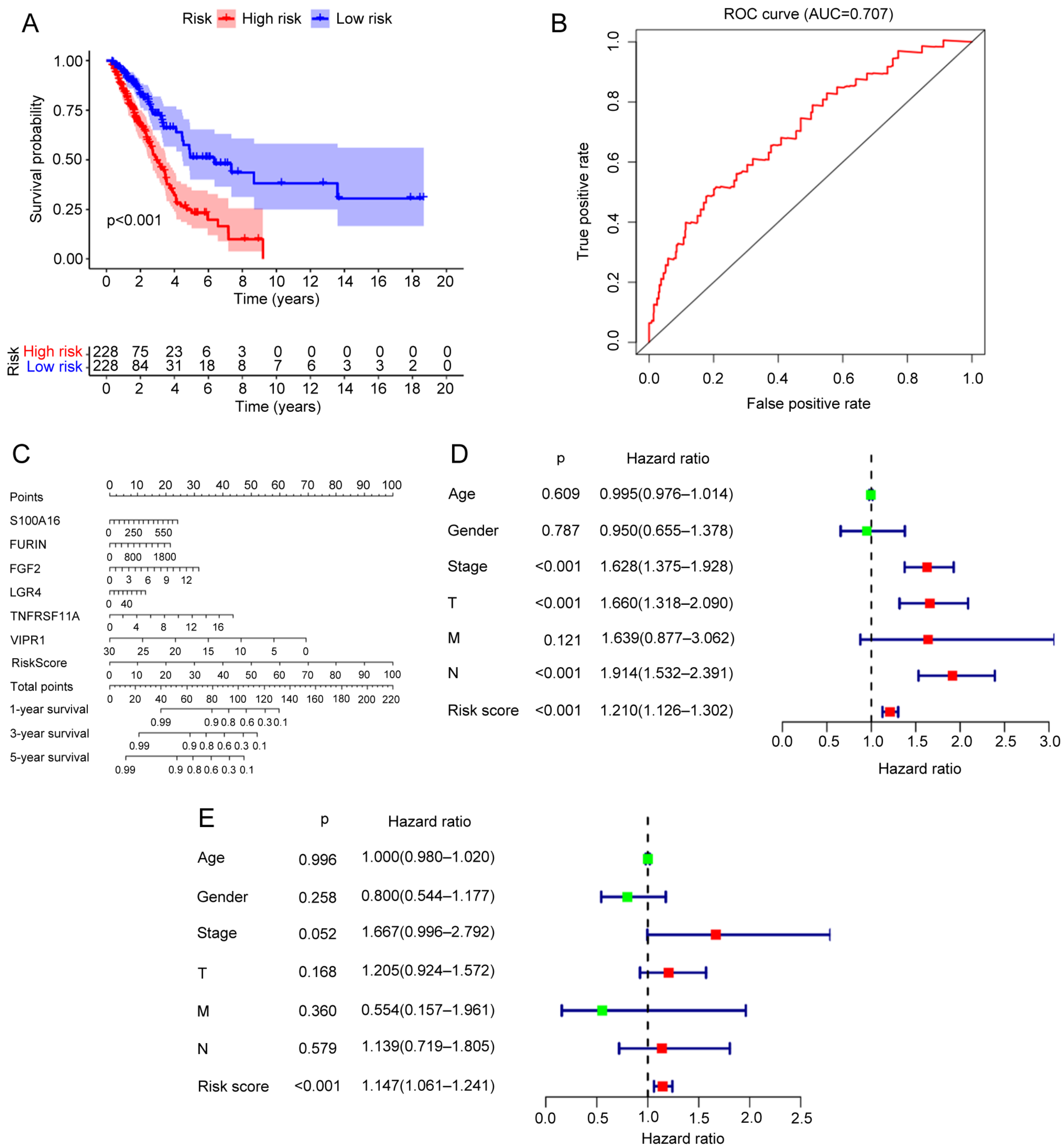

Figure 3. Analysis of prognostic models. (A) Survival curve for high and low risk groups. (B): ROC curve, (C) Nomogram, (D) univariate Cox regression analysis and (E) multivariate Cox regression analysis of the prognostic models. ROC, receiver operating characteristic; AUC, area under the curve.

a straight line between the predicted curve and the total point axis. Moreover, the nomogram could be used to estimate the 1, 3 and 5-year overall survival rates of the patients with LUAD (Fig. 3C) through the predictive power of the prognostic risk model. The univariate Cox regression analysis of the risk score of the prognostic model and the clinical characteristics of LUAD patients (age, sex, stage and TNM scores) revealed that the stage, T, N and risk score all independently predicted the prognosis of patients LUAD (Fig. 3D). Multivariate Cox regression analysis indicated that the risk score independently predicted the prognosis of patients with LUAD (Fig. 3E).

Prognostic immune-related gene expression and survival analysis. The expression levels of *S100A16*, *FURIN*, *LGR4* and *TNFRSF11A* were significantly higher in tumor tissues compared with normal tissues and the expression levels of *VIPR1* and *FGF2* were significantly lower in tumor tissues compared with normal tissues (Fig. 4A-F). Patients with high *S100A16*, *FURIN* and *LGR4* gene expression had a significantly worse prognosis compared with the low expression group, while patients with low *VIPR1* gene expression had a significantly worse prognosis compared with the high expression group. However, *FGF2* and *TNFRSF11A* did not demonstrate a significant impact on the survival time (Fig. 4G-L).

Prognostic gene validation. *S100A16, FURIN*, *LGR4, TNFRSF11A* and *VIPR1* mRNA expression levels were significantly higher in human lung cancer H1975 and A549 cells compared with normal human embryonic lung MRC5 cells. *FURIN* mRNA expression levels were significantly higher in human lung cancer H1975 compared with normal human embryonic lung MRC5 cells. However, *FGF2* expression was significantly lower in the human lung cancer H1975 and A549 cells compared with normal human embryonic lung MRC5 cells (Fig. 5A). Due to the low copy numbers of *S100A16*, *FURIN* and FGF2 in all three cell lines, the significance of gene expression differences between the cell lines should be treated with caution. *S100A16, FURIN, TNFRSF11A* and *VIPR1* were not stained for in normal alveolar tissue cells, with weak/moderate expression in human lung tumor tissue cells. Additionally, *FGF2* staining was weak in normal alveolar and lung tumor tissue cells (Fig. 5B-D). These results indicated the inconsistency of the *VIPR1* expression between LUAD and lung cancer and differences in *FGF2* expression in cell lines and tissues.

Analysis of immune cell infiltration in LUAD. The heat map of immune cell infiltration indicated higher levels of macrophages M0, T cells CD4 memory resting and macrophages M2 cells within LUAD tissue (Fig. 6A). Immune cell component analysis indicated that most immune cells were differentially distributed between the lung adenocarcinoma samples and adjacent tissues (Fig. 6B). The degree of infiltration of B cells naive, plasma cells, T cell CD4 memory activated, T cell follicular helper, T cells regulatory (Tregs), macrophages M2 and dendritic cells resting were significantly higher in lung adenocarcinoma tissue than normal tissues. However degree of infiltration of T cells CD4 memory resting, NK cells resting, macrophages M0, macrophages M1, mast cells resting, eosinophils and neutrophils were significantly lower in lung adenocarcinoma tissue than normal tissues. The correlation between risk genes and immune cells indicated that *FURIN* was significantly positively associated with T cells CD4 memory resting, and significantly negatively associated with T cells regulatory (Tregs), T cells CD8, B cells memory, macrophages M1, dendritic cells resting and mast cells resting. *FGF2* was significantly positively associated with mast cells resting, monocytes, NK cells resting, Tregs and significantly negatively associated with plasma cells and mast cells activated. *TNFRSF11A* was significantly positively associated with macrophages M0 and mast cells resting, and was significantly negatively associated with plasma cells. *VIPR1* was positively associated with dendritic cells activated, macrophages M2, mast cells resting, monocytes, and significantly negatively associated with T cells CD4 memory activated, dendritic cells resting, neutrophils, plasma cells and macrophages M0 (Fig. 6C).

Immune-infiltrating cell survival analysis. The prognosis of patients with LUAD with high expression of macrophages M1, T cells CD4 memory activated, NK cells resting and T cells CD8 activated was significantly worse compared with the low expression group (Fig. 7A-D). However, the low expression of plasma cells, mast cells resting and monocytes indicated a significantly worse prognosis compared with the high expression group (Fig. 7E-G).

Immune-related functional analysis. Antigen presenting cell (APC) co-stimulation, APC co-inhibition, chemokine receptor (CCR), check-point, cytolytic-activity, inflammation-promoting, major histocompatibility complex (MHC)-class-I, parainflammation, T-cell-co-inhibition and Type-I-IFN-Response immune function were expressed at a significantly higher level within the high-risk group (Fig. 8A). Most tumor proliferation-associated function was improved in the high-risk group, which suggested that tumor proliferation was more active (Fig. 8A). The risk model tumor immune escape analysis demonstrated significantly lower TIDE and dysfunction scores within the high-risk group compared with the low-risk group, however the exclusion score was significantly higher in the high-risk group compared with the low-risk group (Fig. 8B-E).

Discussion

Non-small cell lung cancer is the leading cause of lung cancer related deaths worldwide (18). LUAD is the primary lung cancer subtype with specific epidemiological, molecular and clinical features (19). Currently, lung cancer treatment comprises surgery, radiotherapy, chemotherapy (20), targeted drug therapy and immunotherapy (2). For patients with metastatic lung cancer, conventional radiotherapy and chemotherapy may have limited efficacy (21). Tumor immunotherapy is a promising treatment for use following surgery, radiotherapy, chemotherapy or targeted therapy. Previous clinical studies have reported that many tumors are insensitive to immunotherapy due to the immune tumor microenvironment, with immune genes serving a vital role in this insensitivity. Previous studies have reported that CD3, IL-12 and IL-17 expression in the tumor stroma is significantly linked with postoperative recurrence of early LUAD (22-24). Furthermore,

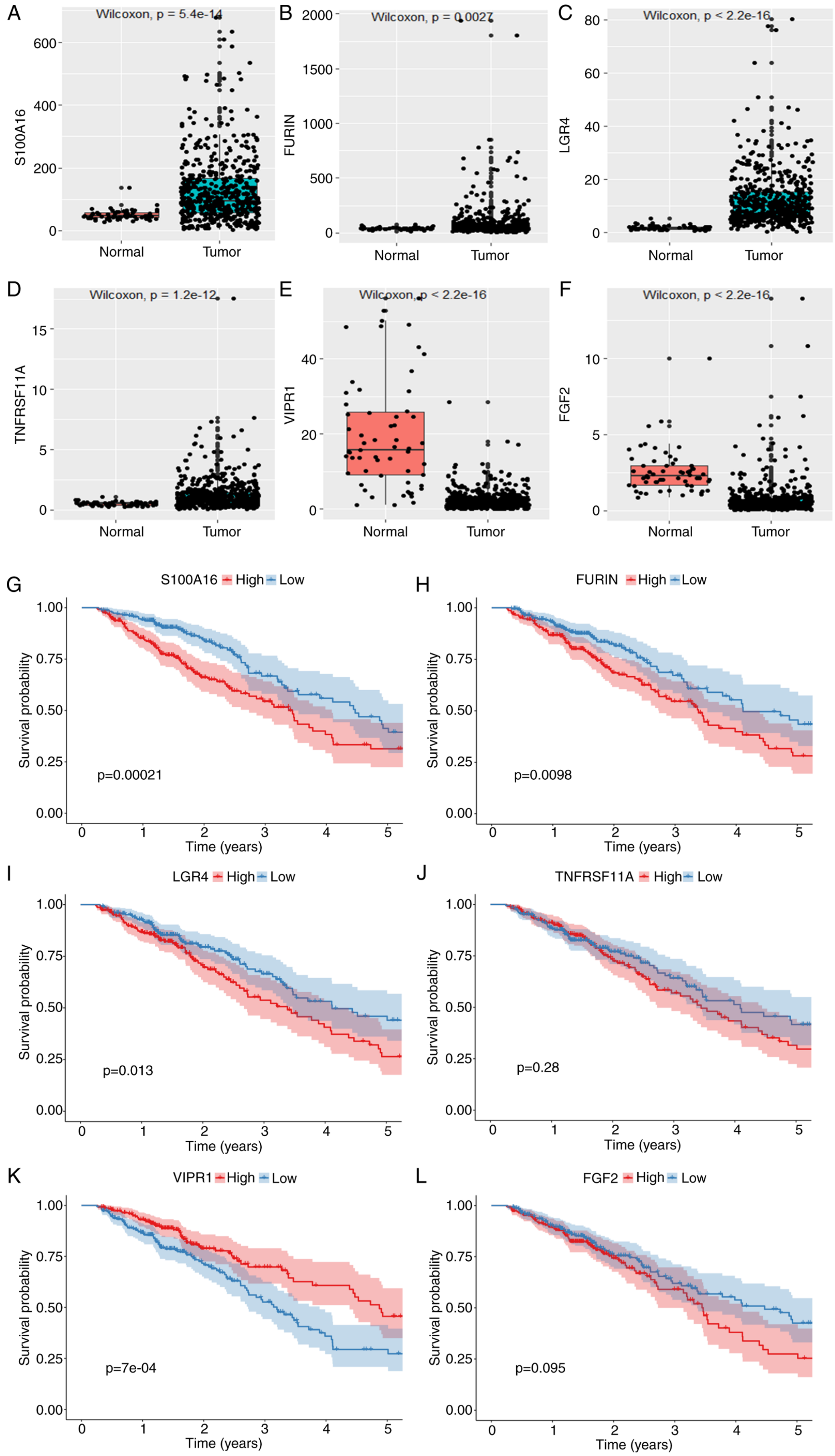

Figure 4. Prognostic gene expression and survival analysis. Expression of (A) S100A16, (B) FURIN, (C) LGR4, (D) TNFRSF11A, (E) VIPR1 and (F) FGF2 in normal and tumor tissues. Survival analysis of patients with high and low expression levels of (G) S100A16, (H) FURIN, (I) LGR4, (J) TNFRSF11A, (K) VIPR1 and (L) FGF2.

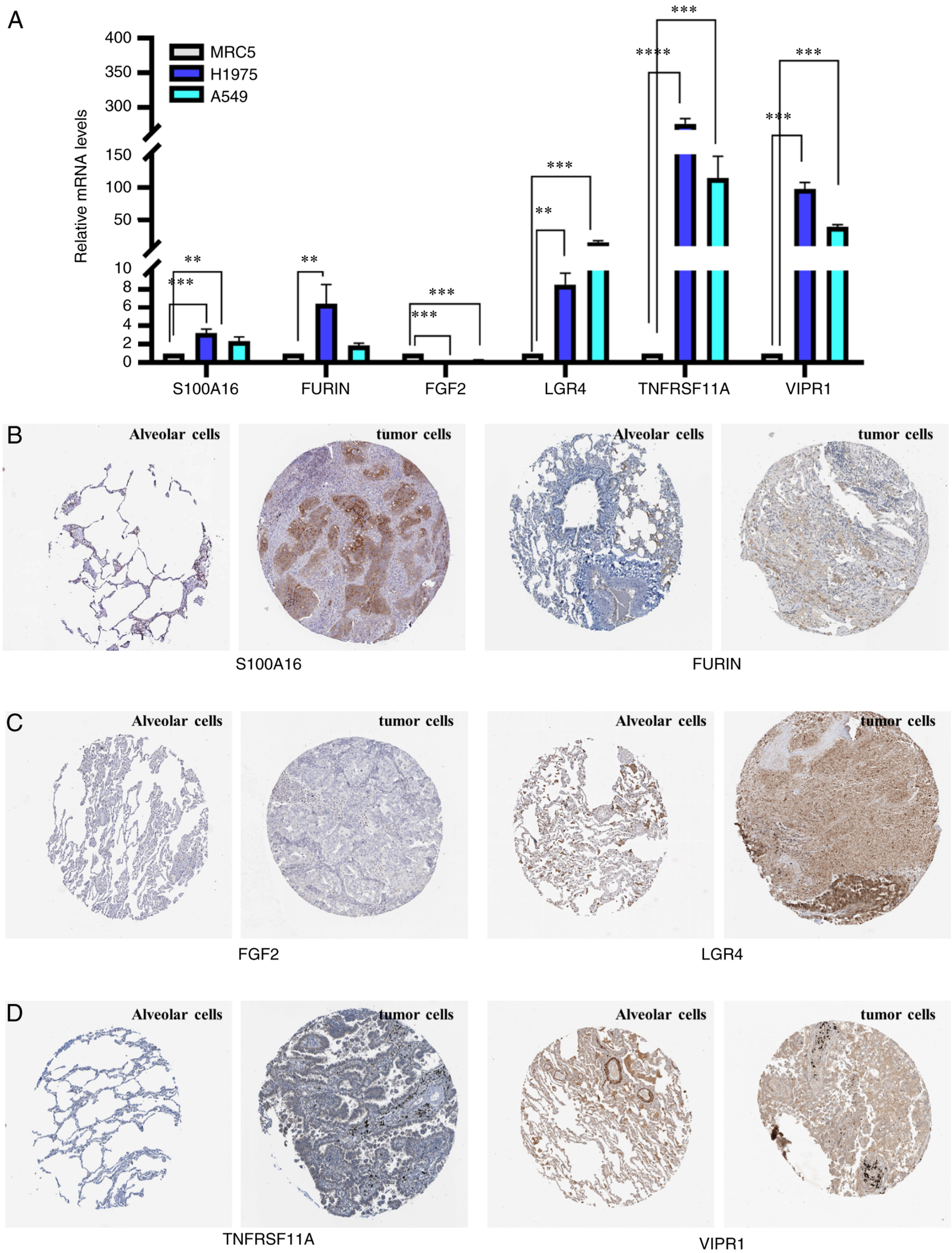

Figure 5. Reverse transcription-quantitative PCR and staining analysis. (A) S100A16, FURIN, FGF2, LGR4, TNFRSF11A and VIPR1 mRNA expression levels in MRC5, H1975 and A549 cells. (B) S100A16, FURIN, (C) FGF2, LGR4, (D) TNFRSF11A, and VIPR1 protein expression in normal alveolar and tumor cells. The immunohistochemistry images were downloaded from the Human Protein Atlas database (https://www.proteinatlas.org/ENSG00000188643-S100A16/pathology/lung+cancer; https://www.proteinatlas.org/ENSG00000140564-FURIN/pathology/lung+cancer; https://www.proteinatlas.org/ENSG00000205213-LGR4/pathology/lung+cancer; https://www.proteinatl-as.org/ENSG00000141655-TNFRSF11A/pathology/lung+cancer; and https://www.proteina-tlas.org/ENSG00000114812-VIPR1/pathology/lung+cancer). **P<0.01, ***P<0.001 and ****P<0.0001.

many immune factors and cells (such as, neutrophils, macrophages and lymphocytes) are associated with angiogenesis, cell proliferation and invasion in LUAD (25). Therefore, the elucidation of immune-related genes with biological significance and assessment of their prognostic value could aid the diagnosis and treatment of patients with LUAD.

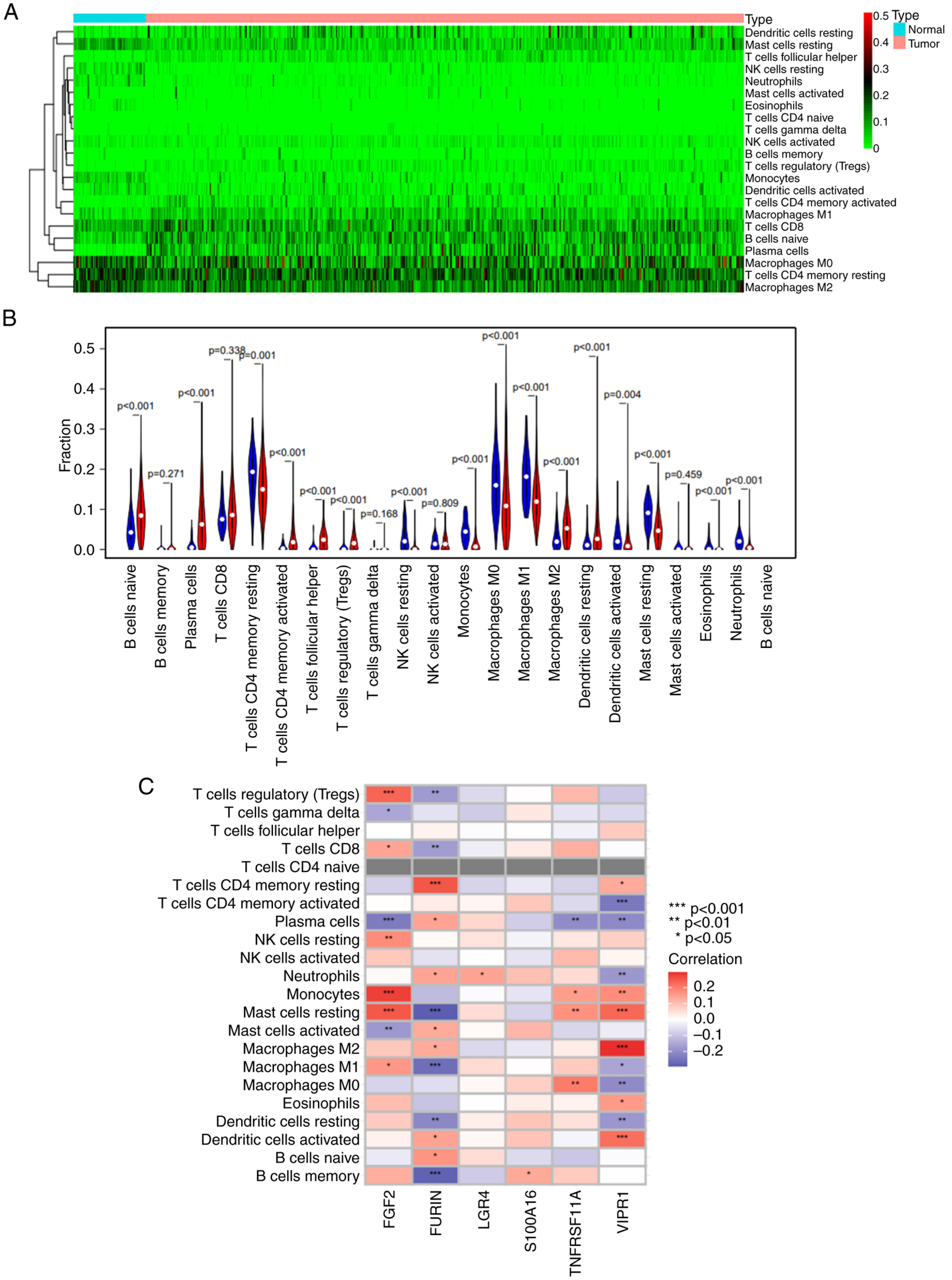

Figure 6. Analysis of immune cell infiltration. (A) Immune cell types involved in lung adenocarcinoma represented using a heat map. Red indicates high expression and green indicates low expression. (B) Differential expression of immune cells. blue indicates normal tissue and red indicates tumor tissue. (C) Correlation between prognostic genes and infiltrating immune cells. *P<0.05, **P<0.01 and ***P<0.001.

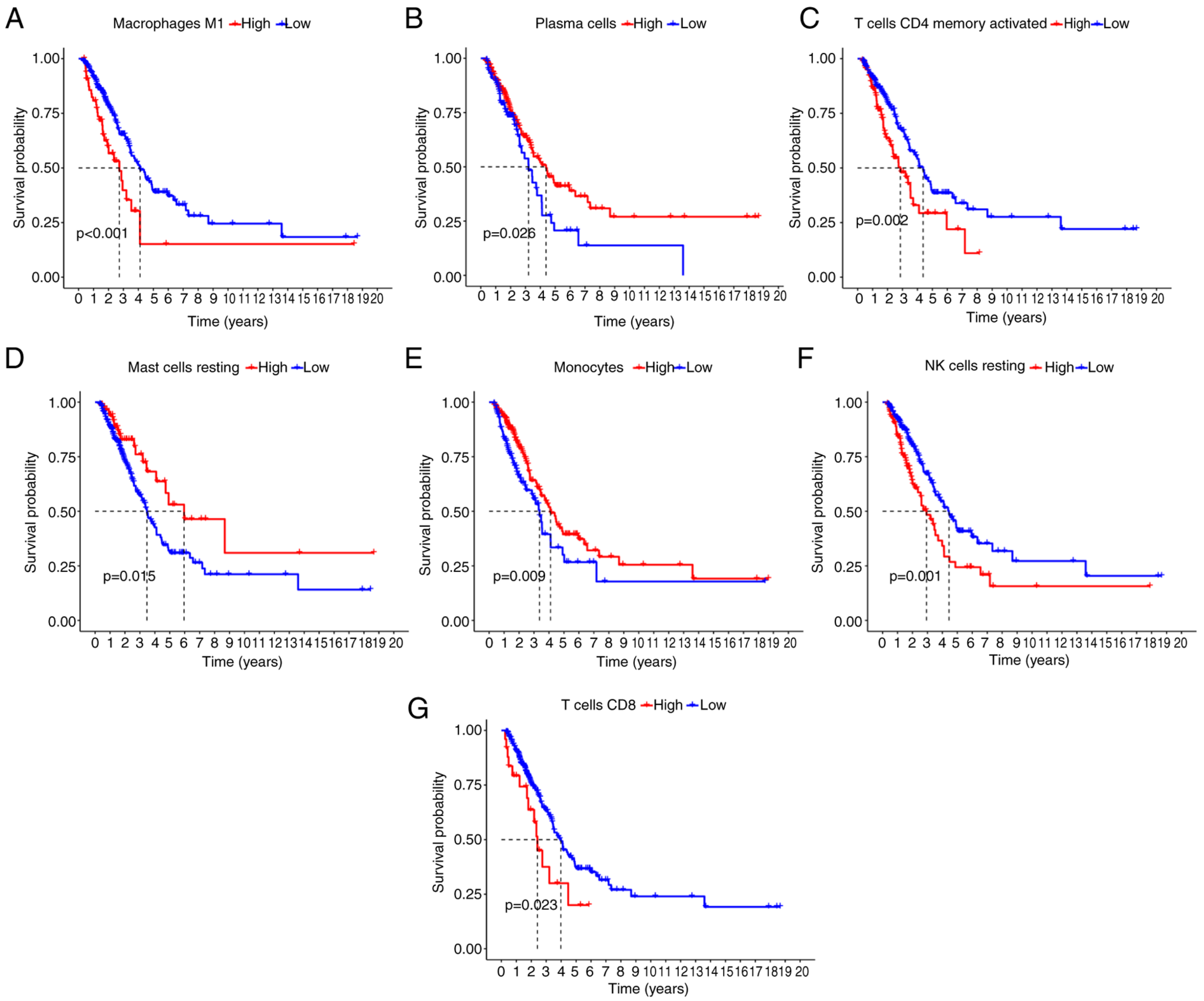

Figure 7. Immune cell survival analysis. Survival analysis of patients with high and low expression of (A) macrophages M1, (B) T cells CD4 memory activated, (C) NK cells resting, (D) T cells CD8, (E) plasma cells, (F) mast cells resting and (G) monocytes.

Previous studies have demonstrated that abnormally expressed genes can be utilized as prognostic LUAD markers (26-28). However, only a few previous studies have reported the abnormally expressed immune genes and their immune infiltration role (29-31). The present study first identified six immune-related genes closely related to the prognosis of LUAD patients, including *S100A16*, *FURIN*, *FGF2*, *LGR4*, *TNFRSF11A* and *VIPR1*. These genes serve an important biological role in the occurrence and development of tumors. Among these genes, *S100A16* is highly conserved in mammals (32), and its high expression is linked with tumor cell growth and EMT (33). *S100A16* is a prognostic marker for various tumors, including LUAD and colorectal cancer (34,35). The present study showed that *S100A16* was highly expressed in NSCLC cells and that its high expression was associated with a worse prognosis in LUAD. *FURIN* is a protein conversion enzyme expressed in breast cancer, squamous cell carcinoma and striated muscle tumors, which indicates that it may hold an important role. *FURIN* expression is elevated in NSCLC, and upregulated RURIN activity correlates with accelerated tumor progression (36,37). The present study found high *FURIN* expression was associated with a worse prognosis in patients with LUAD and with an increased number of infiltrated immune cells. *FGF2* is a fibroblast growth factor family member and exerts mitogenic activity by binding to fibroblast factor receptors (38). It is a tumor angiogenesis factor, and neutrophils are reported to enhance the growth of liver metastases through FGF2-dependent angiogenesis, converting tumor-associated macrophages into pro-tumorigenic M2 macrophages (39). The present study demonstrated that the low *FGF2* expression in LUAD cells was closely linked with increased numbers of infiltrated immune cells. *LGR4* is a receptor of the G protein-coupled receptors superfamily, which regulate signaling pathways in normal and pathological processes. *LGR4* is commonly activated by R-spondins, Norrin and receptor activators of NF-κβ ligand. *LGR4* activation leads to signaling in the Wnt/β-catenin and G protein-associated pathways (40). *LGR4* is highly expressed in several cancers, enhances tumorigenesis and metastasis, regulates cancer stem cells and is linked with poor patient

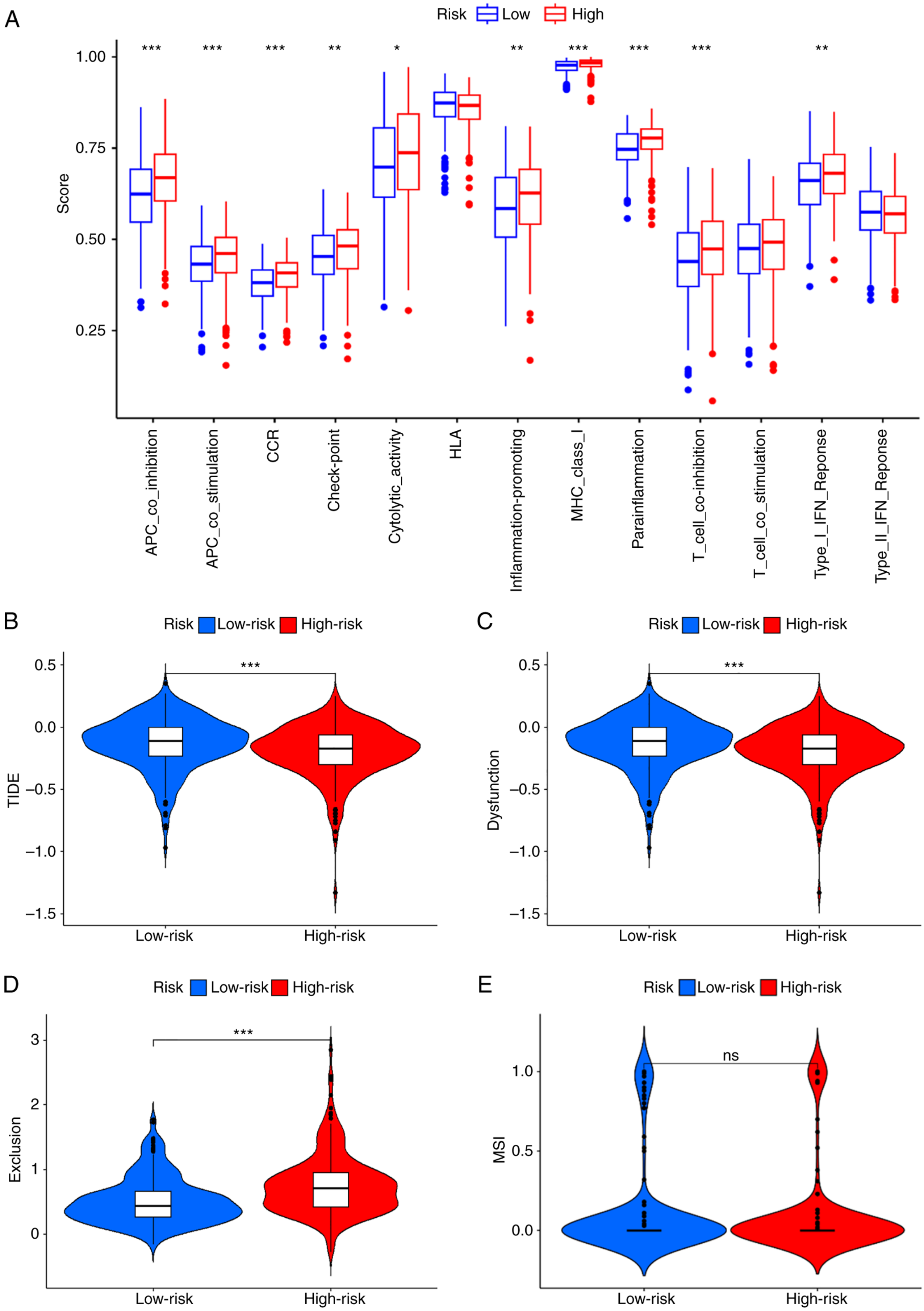

Figure 8. Immune-related functional analysis. (A) The scores of 13 immune-related functions among high and low-risk groups of LUAD. (B) TIDE, (C) Dysfunction, (D) Exclusion and (E) MSI scores for high and low-risk groups of patients with LUAD. TIDE, Tumor Immune Dysfunction and Exclusion; MSI, microsatellite instability; LUAD, lung adenocarcinoma. *P<0.05, **P<0.01 and ***P<0.001.

prognosis (41-43). The present study showed a high level of *LGR4* expression in NSCLC cells, with a worse prognosis for patients with LUAD. *TNFRSF11A* is a crucial regulator of cell differentiation, proliferation and survival, an inducer for the activation of dendritic cells, and a critical factor in maintaining immune tolerance (44). *TNFRSF11A* promotes cervical cancer cell proliferation and inhibits cell apoptosis (45). The present study showed high T*NFRSF11A* expression in LUAD cells which was related to increased infiltrated immune cells. *VIP* is a vital neuropeptide controlling lung physiology and mainly functions through two receptor subtypes, *VAPC1* and *VAPC2* (46). *VIP* or *VPAC1* receptor antagonist strengthens the ability of chemotherapy to kill breast cancer cells (47) while improving anti-viral immunity (48). *VIPR1* inhibits the growth of certain cancers including prostate cancer and lymphoblastoma, and *VIPR1* overexpression inhibits the proliferation of LUAD H1299 cells (49). The present study found a low *VIPR1* expression in LUAD cells, which was associated with infiltrated immune cells, and patients with low expression of VIPR1 had a worse prognosis.

The prognostic risk model generated in the present study depicted significant prognostic differences between the high and low-risk groups. Immune cell infiltration, immune cell-related functions and TIDE were compared in high and low-risk patient groups to elucidate the potential reasons behind the prognostic differences. We jypothesize that the differences in the degree of tumor immune cell infiltration, immune-related functions and low TIDE score may be potential mechanisms affecting the prognosis of patients with LUAD. The present study indicated that immune cells, including T cells CD4 memory resting, T cells CD8, macrophages M0, macrophages M1, plasma cells and B cells naive were dominant in both LUAD and normal tissue. Thus, monocyte macrophages, NK cells resting and T cells follicular helper were also expressed in LUAD. Macrophages M1 and M2 are crucial immune cells polarized by circulating monocytes (50). Macrophages M1 generate reactive oxygen/nitrogen species and pro-inflammatory factors critical for host defense and tumor cell death. The increase in the levels of macrophages M1 has been reported to promote the tumor-antagonistic effect of M1-polarized macrophages and enhances the survival trend of colorectal cancer patients (51). However, macrophages M2 promote angiogenesis and matrix remodeling, which enhance tumor progression and metastasis, and suppress immune surveillance of tumor cells (52). Although NK cells are essential for tumor immune surveillance, a previous study reported that their ability to kill target cells and produce IFN-γ may be decreased in NSCLC tumors (53). The current study demonstrated that levels of NK cells activated were lower in LUAD; thus, infiltrating NK cells is inhibited. NK cells resting in normal tissues express more without releasing their toxic particles before non-specific target cell recognition. In recent years, increasing evidence has demonstrated effective interaction between NK cells and B cells (54). Although B cells can release cytokines with cytotoxic T-cell activity and function as effective antigen-presenting cells, their anti-tumor role in the TME remains debatable. Nevertheless, previous studies have described that B cells can recruit myeloid-derived suppressor cells, improve vascular survival by producing cytokines (55) and potentially induce tumors by blocking cytotoxic T lymphocyte function (56).

Immune function scores, including APC-co-inhibition, APC co-stimulation, CCR, MHC-class-I, parainflammation and T-cell-co-inhibition were significantly elevated in the high-risk group. Thus, the density of immune dysfunction was higher, with a worse prognosis in the high-risk group. The present study also assessed the difference in TIDE scores between high and low-risk groups, and the result showed the high-risk group with a lower TIDE score. TIDE analysis focuses on the function and status of T cells without reflecting the complexity of the immune cell infiltration in the TME which is associated with immunotherapy responses (57). However, TIDE can predict patient response to immunotherapy (58). The TIDE score calculates the efficacy of ICIs for treating tumors. A high TIDE score indicates poor ICI efficacy with a short survival period post-ICI treatment. The current study demonstrated a low TIDE score within the prognostic model for the high-risk group. Thus, LUAD tumors of the high-risk group are less likely to escape immune killing, enhancing their treatment using better immunotherapy. Higher TIDE scores are linked with a greater likelihood of immune evasion and reduced survival in patients receiving ICIs, rendering immunotherapy less effective (14). The low-risk group had higher immune evasion potential. This indicated that the high-risk group could derive greater benefit from immunotherapy with an improved prognosis.

The current study has certain limitations. First, some of the roles and mechanisms of genes in the LUAD model remain unclear. Therefore, further experiments are required to assess their functions and mechanisms. Second, the study data came from public databases and most patients did not receive immunotherapy. Deficiencies also exist in predicting the prognosis of lung cancer patients who underwent immunotherapy, highlighting the need for additional clinical samples. Third, these results were primarily obtained using bioinformatic analysis and lack clinical, *in vitro* and *in vivo* studies to support the results.

In conclusion, the present study identified six immune-related genes linked with patient prognosis, and a prognostic risk model was constructed for LUAD based on bioinformatic analysis. The survival times of patients with LUAD could be independently predicted using the prognostic risk model. It is anticipated that future treatments for LUAD molecular targets will require targeting of these genes to guide the diagnosis and treatment of LUAD patients.

Acknowledgments

The authors would like to thank Ms. Mao Yang, Miss Wenjun Wang and Miss Xianyu Zhu (Institute for Cancer Medicine, School of Basic Medicine Sciences, Southwest Medical University, Luzhou, Sichuan, China) for their support in performing experiments.

Funding

The present study was supported by the Sichuan Science and Technology Program (grant no. 2022YFS0623), the Sichuan Science and Technology Program Joint Innovation

Grant (grant no. 2022YFS0623-B3), Southwest Medical University Grant (grant no. 2021ZKZD005) and Sichuan Science and Technology Grant (grant no. 2020YFH0121).

Availability of data and materials

The data generated in the present study may be requested from the corresponding author.

Authors' contributions

JY and WY designed the study, drafted the manuscript and confirm the authenticity of all the raw data. JY performed TCGA data analysis and drew the figures. CT performed the cellular experiments and qPCR, and analyzed the data. CL helped perform the cellular experiments and analyzed the data. XL helped design the study, provided the cells and critically revised the drafted work for content. All the authors read and approved the final version of the manuscript.

Ethics approval and consent to participate

Not applicable.

Patient consent for publication

Not applicable.

Competing interests

The authors declare that they have no competing interests.

References

1. Sung H, Ferlay J, Siegel RL, Laversanne M, Soerjomataram I, Jemal A and Bray F: Global cancer statistics 2020: GLOBOCAN estimates of incidence and mortality worldwide for 36 cancers in 185 countries. CA Cancer J Clin 71: 209-249, 2021.
2. Lahiri A, Maji A, Potdar PD, Singh N, Parikh P, Bisht B, Mukherjee A and Paul MK: Lung cancer immunotherapy: progress, pitfalls, and promises. Mol Cancer 22: 40, 2023.
3. Shi J, Hua X, Zhu B, Ravichandran S, Wang M, Nguyen C, Brodie SA, Palleschi A, Alloisio M, Pariscenti G, *et al*: Somatic genomics and clinical features of lung adenocarcinoma: A retrospective study. PLoS Med 13: e1002162, 2016.
4. Ortega MA, Pekarek L, Navarro F, Fraile-Martínez O, García-Montero C, Álvarez-Mon MÁ, Diez-Pedrero R, Boyano-Adánez MDC, Guijarro LG, Barrena-Blázquez S, *et al*: Updated views in targeted therapy in the patient with non-small cell lung cancer. J Pers Med 13: 167, 2023.
5. Byun J, Schwartz AG, Lusk C, Wenzlaff AS, de Andrade M, Mandal D, Gaba C, Yang P, You M, Kupert EY, *et al*: Genome-wide association study of familial lung cancer. Carcinogenesis 39: 1135-1140, 2018.
6. Schreiber RD, Old LJ and Smyth MJ: Cancer immunoediting: Integrating immunity's roles in cancer suppression and promotion. Science 331: 1565-1570, 2011.
7. Joyce JA and Fearon DT: T cell exclusion, immune privilege, and the tumor microenvironment. Science 348: 74-80, 2015.
8. Karasaki T, Nagayama K, Kuwano H, Nitadori JI, Sato M, Anraku M, Hosoi A, Matsushita H, Morishita Y, Kashiwabara K, *et al*: An immunogram for the cancer-immunity cycle: Towards personalized immunotherapy of lung cancer. J Thorac Oncol 12: 791-803, 2017.
9. Liede A, Hernandez RK, Wade SW, Bo R, Nussbaum NC, Ahern E, Dougall WC and Smyth MJ: An observational study of concomitant immunotherapies and denosumab in patients with advanced melanoma or lung cancer. Oncoimmunology 7: e1480301, 2018.
10. Mahalingam P and Newsom-Davis T: Cancer immunotherapy and the management of side effects. Clin Med (Lond) 23: 56-60, 2023.
11. Luo W: Nasopharyngeal carcinoma ecology theory: Cancer as multidimensional spatiotemporal 'unity of ecology and evolution' pathological ecosystem. Theranostics 13: 1607-1631, 2023.
12. Yang Y, Yu Y and Lu S: Effectiveness of PD-1/PD-L1 inhibitors in the treatment of lung cancer: Brightness and challenge. Sci China Life Sci 63: 1499-1514, 2020.
13. Zhang S, Zeng Z, Liu Y, Huang J, Long J, Wang Y, Peng X, Hu Z and Ouyang Y: Prognostic landscape of tumor-infiltrating immune cells and immune-related genes in the tumor microenvironment of gastric cancer. Aging (Albany NY) 12: 17958-17975, 2020.
14. Jiang P, Gu S, Pan D, Fu J, Sahu A, Hu X, Li Z, Traugh N, Bu X, Li B, *et al*: Signatures of T cell dysfunction and exclusion predict cancer immunotherapy response. Nat Med 24: 1550-1558, 2018.
15. Yu G, Wang LG, Han Y and He QY: clusterProfiler: An R package for comparing biological themes among gene clusters. OMICS 16: 284-287, 2012.
16. Heagerty PJ, Lumley T and Pepe MS: Time-dependent ROC curves for censored survival data and a diagnostic marker. Biometrics 56: 337-344, 2000.
17. Livak KJ and Schmittgen TD: Analysis of relative gene expression data using real-time quantitative PCR and the 2(-Delta Delta C(T)) method. Methods 25: 402-408, 2001.
18. Li S, Zhu R, Li D, Li N and Zhu X: Prognostic factors of oligometastatic non-small cell lung cancer: A meta-analysis. J Thorac Dis 10: 3701-3713, 2018.
19. Ortega MA, Navarro F, Pekarek L, Fraile-Martínez O, García-Montero C, Saez MA, Arroyo M, Monserrat J and Alvarez-Mon M: Exploring histopathological and serum biomarkers in lung adenocarcinoma: Clinical applications and translational opportunities (review). Int J Oncol 61: 154, 2022.
20. Leduc C, Antoni D, Charloux A, Falcoz PE and Quoix E: Comorbidities in the management of patients with lung cancer. Eur Respir J 49: 1601721, 2017.
21. Fan T, Lu J, Niu D, Zhang Y, Wang B, Zhang B, Zhang Z, He X, Peng N, Li B, *et al*: Immune and non-immune cell subtypes identify novel targets for prognostic and therapeutic strategy: A study based on intratumoral heterogenicity analysis of multicenter scRNA-seq datasets in lung adenocarcinoma. Front Immunol 13: 1046121, 2022.
22. Airoldi I, Di Carlo E, Cocco C, Caci E, Cilli M, Sorrentino C, Sozzi G, Ferrini S, Rosini S, Bertolini G, *et al*: IL-12 can target human lung adenocarcinoma cells and normal bronchial epithelial cells surrounding tumor lesions. PLoS One 4: e6119, 2009.
23. Huang Q, Duan L, Qian X, Fan J, Lv Z, Zhang X, Han J, Wu F, Guo M, Hu G, *et al*: IL-17 promotes angiogenic factors IL-6, IL-8, and Vegf production via Stat1 in lung adenocarcinoma. Sci Rep 6: 36551, 2016.
24. Suzuki K, Kadota K, Sima CS, Nitadori J, Rusch VW, Travis WD, Sadelain M and Adusumilli PS: Clinical impact of immune microenvironment in stage I lung adenocarcinoma: Tumor interleukin-12 receptor β2 (IL-12Rβ2), IL-7R, and stromal FoxP3/CD3 ratio are independent predictors of recurrence. J Clin Oncol 31: 490-498, 2013.
25. Domagala-Kulawik J, Kwiecien I, Pankowski J, Pasieka-Lis M, Wolosz D and Zielinski M: Elevated Foxp3/CD8 ratio in lung adenocarcinoma metastatic lymph nodes resected by transcervical extended mediastinal lymphadenectomy. Biomed Res Int 2017: 5185034, 2017.
26. Ma C, Li F, Wang Z and Luo H: A novel immune-related gene signature predicts prognosis of lung adenocarcinoma. Biomed Res Int 2022: 4995874, 2022.
27. Wu X, Zhu J, Liu W, Jin M, Xiong M and Hu K: A novel prognostic and predictive signature for lung adenocarcinoma derived from combined hypoxia and infiltrating immune cell-related genes in TCGA patients. Int J Gen Med 14: 10467-10481, 2021.
28. Yang D, Ma X and Song P: A prognostic model of non small cell lung cancer based on TCGA and ImmPort databases. Sci Rep 12: 437, 2022.
29. Sun L, Zhang Z, Yao Y, Li WY and Gu J: Analysis of expression differences of immune genes in non-small cell lung cancer based on TCGA and ImmPort data sets and the application of a prognostic model. Ann Transl Med 8: 550, 2020.
30. Sun S, Guo W, Wang Z, Wang X, Zhang G, Zhang H, Li R, Gao Y, Qiu B, Tan F, *et al*: Development and validation of an immune-related prognostic signature in lung adenocarcinoma. Cancer Med 9: 5960-5975, 2020.

31. Qi C, Ma J, Sun J, Wu X and Ding J: The role of molecular subtypes and immune infiltration characteristics based on disulfidptosis-associated genes in lung adenocarcinoma. Aging (Albany NY) 15: 5075-5095, 2023.
32. Babini E, Bertini I, Borsi V, Calderone V, Hu X, Luchinat C and Parigi G: Structural characterization of human S100A16, a low-affinity calcium binder. J Biol Inorg Chem 16: 243-256, 2011.
33. Basnet S, Vallenari EM, Maharjan U, Sharma S, Schreurs O and Sapkota D: An update on S100A16 in human cancer. Biomolecules 13: 1070, 2023.
34. Chen D, Luo L and Liang C: Aberrant S100A16 expression might be an independent prognostic indicator of unfavorable survival in non-small cell lung adenocarcinoma. PLoS One 13: e0197402, 2018.
35. Sun X, Wang T, Zhang C, Ning K, Guan ZR, Chen SX, Hong TT and Hua D: S100A16 is a prognostic marker for colorectal cancer. J Surg Oncol 117: 275-283, 2018.
36. Bassi DE, Mahloogi H, Al-Saleem L, Lopez De Cicco R, Ridge JA and Klein-Szanto AJ: Elevated furin expression in aggressive human head and neck tumors and tumor cell lines. Mol Carcinog 31: 224-232, 2001.
37. Braun E and Sauter D: Furin-mediated protein processing in infectious diseases and cancer. Clin Transl Immunology 8: e1073, 2019.
38. Babina IS and Turner NC: Advances and challenges in targeting FGFR signalling in cancer. Nat Rev Cancer 17: 318-332, 2017.
39. Im JH, Buzzelli JN, Jones K, Franchini F, Gordon-Weeks A, Markelc B, Chen J, Kim J, Cao Y and Muschel RJ: FGF2 alters macrophage polarization, tumour immunity and growth and can be targeted during radiotherapy. Nat Commun 11: 4064, 2020.
40. Gong X, Yi J, Carmon KS, Crumbley CA, Xiong W, Thomas A, Fan X, Guo S, An Z, Chang JT and Liu QJ: Aberrant RSPO3-LGR4 signaling in Keap1-deficient lung adenocarcinomas promotes tumor aggressiveness. Oncogene 34: 4692-4701, 2015.
41. Luo J, Yang Z, Ma Y, Yue Z, Lin H, Qu G, Huang J, Dai W, Li C, Zheng C, *et al*: LGR4 is a receptor for RANKL and negatively regulates osteoclast differentiation and bone resorption. Nat Med 22: 539-546, 2016.
42. Glinka A, Dolde C, Kirsch N, Huang YL, Kazanskaya O, Ingelfinger D, Boutros M, Cruciat CM and Niehrs C: LGR4 and LGR5 are R-spondin receptors mediating Wnt/β-catenin and Wnt/PCP signalling. EMBO Rep 12: 1055-1061, 2011.
43. Ruffner H, Sprunger J, Charlat O, Leighton-Davies J, Grosshans B, Salathe A, Zietzling S, Beck V, Therier M, Isken A, *et al*: R-Spondin potentiates Wnt/β-catenin signaling through orphan receptors LGR4 and LGR5. PLoS One 7: e40976, 2012.
44. Ono T, Hayashi M, Sasaki F and Nakashima T: RANKL biology: Bone metabolism, the immune system, and beyond. Inflamm Regen 40: 2, 2020.
45. Shang WQ, Li H, Liu LB, Chang KK, Yu JJ, Xie F, Li MQ and Yu JJ: RANKL/RANK interaction promotes the growth of cervical cancer cells by strengthening the dialogue between cervical cancer cells and regulation of IL-8 secretion. Oncol Rep 34: 3007-3016, 2015.
46. Szilasi M, Buglyo A, Treszl A, Kiss L, Schally AV and Halmos G: Gene expression of vasoactive intestinal peptide receptors in human lung cancer. Int J Oncol 39: 1019-1024, 2011.
47. Moody TW, Leyton J, Chan D, Brenneman DC, Fridkin M, Gelber E, Levy A and Gozes I: VIP receptor antagonists and chemotherapeutic drugs inhibit the growth of breast cancer cells. Breast Cancer Res Treat 68: 55-64, 2001.
48. Yassin MA, Datiko DG, Tulloch O, Markos P, Aschalew M, Shargie EB, Dangisso MH, Komatsu R, Sahu S, Blok L, *et al*: Innovative community-based approaches doubled tuberculosis case notification and improve treatment outcome in Southern Ethiopia. PLoS One 8: e63174, 2013.
49. Zhao L, Yu Z and Zhao B: Mechanism of VIPR1 gene regulating human lung adenocarcinoma H1299 cells. Med Oncol 36: 91, 2019.
50. Tong Z, Wang X, Liu H, Ding J, Chu Y and Zhou X: The relationship between tumor infiltrating immune cells and the prognosis of patients with lung adenocarcinoma. J Thorac Dis 15: 600-610, 2023.
51. Aras S and Zaidi MR: TAMeless traitors: Macrophages in cancer progression and metastasis. Br J Cancer 117: 1583-1591, 2017.
52. Wolf D, Sopper S, Pircher A, Gastl G and Wolf AM: Treg(s) in cancer: Friends or foe? J Cell Physiol 230: 2598-2605, 2015.
53. Platonova S, Cherfils-Vicini J, Damotte D, Crozet L, Vieillard V, Validire P, André P, Dieu-Nosjean MC, Alifano M, Régnard JF, *et al*: Profound coordinated alterations of intratumoral NK cell phenotype and function in lung carcinoma. Cancer Res 71: 5412-5422, 2011.
54. Yuan D, Koh CY and Wilder JA: Interactions between B lymphocytes and NK cells. FASEB J 8: 1012-1018, 1994.
55. Garaud S, Buisseret L, Solinas C, Gu-Trantien C, de Wind A, Van den Eynden G, Naveaux C, Lodewyckx JN, Boisson A, Duvillier H, *et al*: Tumor infiltrating B-cells signal functional humoral immune responses in breast cancer. JCI Insight 5: e129641, 2019.
56. Tsou P, Katayama H, Ostrin EJ and Hanash SM: The emerging role of B cells in tumor immunity. Cancer Res 76: 5597-5601, 2016.
57. Tian J, Fu C, Peng Q, Yang J, Fan X, Zeng X, Qing W and Wu Y: Construction of immune cell infiltration score model to assess prognostic ability of tumor immune environment in lung adenocarcinoma. Am J Transl Res 15: 1730-1743, 2023.
58. Chen C, Huang H and Wu CH: Protein bioinformatics databases and resources. Methods Mol Biol 694: 3-24, 2011.